Influence of the substrate misorientation on the properties of N-polar InGaN/GaN and AlGaN/GaN heterostructures

S. Keller,[a] C. S. Suh, N. A. Fichtenbaum, M. Furukawa, R. Chu, Z. Chen, K. Vijayraghavan, S. Rajan, S. P. DenBaars, J. S. Speck, and U. K. Mishra
Electrical and Computer Engineering Department and Materials Department, University of California, Santa Barbara, California 93106, USA

(Received 8 July 2008; accepted 9 September 2008; published online 5 November 2008)

Smooth N-polar InGaN/GaN and AlGaN/GaN multiquantum wells (MQWs) and heterostructures were grown by metal organic chemical vapor deposition on (0001) sapphire substrates with misorientation angles of 2°–5° toward the *a*-sapphire plane. For all investigated structures the tendency toward formation of multiatomic steps at the film surface and at interfaces increased with increasing misorientation angle. Thereby the crystal misorientation led to a stronger degradation of the interface quality and periodicity of InGaN/GaN in comparison to the AlGaN/GaN MQWs. While the alloy composition of AlGaN films was unaffected by the misorientation, the indium mole fraction in the InGaN layers and the wavelength of the MQW related luminescence decreased with increasing misorientation angle. The properties of the two dimensional electron gas (2DEG), which formed at the upper interface of semi-insulating GaN/AlGaN/GaN heterostructures, were strongly anisotropic. Whereas the resistivity of the 2DEG measured perpendicular to the surface steps/undulations decreased with increasing misorientation angle, the resistivity measured in the parallel direction was significantly lower and unaffected by the crystal misorientation. Electron mobility values as high as 1800 $cm^2/V\,s$ were determined for conduction parallel to the surface steps/undulations. © *2008 American Institute of Physics*. [DOI: 10.1063/1.3006132]

I. INTRODUCTION

While the properties of Ga-polar (Al,In,Ga)N/GaN structures have been widely studied in the past, N-polar nitride films were much less investigated, largely related to difficulties in the growth of smooth N-polar films, in particular by metal organic chemical vapor deposition (MOCVD). In contrast to group-III metal polar films grown in the typical $\langle 0001 \rangle$ direction, which can be fabricated in high quality using a variety of growth techniques leading to the development of GaN based high efficiency light emitting diodes, laser diodes, and high power transistors, N-polar GaN films (growth direction $\langle 000\bar{1} \rangle$) often exhibited hexagonal hillocks hampering their application for devices.[1,2] Due to the hexagonal symmetry of the GaN crystal, the properties of (Al,Ga,In)N heterostructures grown in both directions are strongly influenced by polarization effects, resulting in strong electric fields in the crystal.[2–4] The opposite direction of the electric fields in N-polar in comparison to Ga-polar heterostructures is interesting for a variety of device applications, for example enhancement mode transistors and highly scaled transistors, photodetectors, and solar cells. After problems in the growth of N-polar GaN were overcome by molecular beam epitaxy (MBE) using C-polar SiC as substrate,[5] the first (Al,Ga)N/GaN field effect transistors (FETs) were demonstrated.[6,7] There are, however, only a few reports on the growth of smooth N-polar GaN layers by MOCVD.[8–10] Recently, we fabricated high quality N-polar GaN films and GaN/AlGaN/GaN structures for FET applications by MOCVD using misoriented sapphire substrates.[11,12] In this study we investigated the relationship between substrate misorientation angle and the properties of N-polar AlGaN/GaN and InGaN/GaN heterostructures using (Al,Ga,In)N/GaN multiquantum well (MQW) samples and GaN/AlGaN/GaN heterostructures.

II. EXPERIMENT

In all experiments (0001) sapphire substrates with misorientation angles of 2°, 3°, 4°, and 5° toward the *a*-sapphire plane were coloaded. The misorientation toward the *a*-sapphire plane was chosen as smoother GaN films with a more regular surface morphology were realized in previous experiments on substrates misoriented toward the *a* in comparison to the *m*-sapphire plane, particularly at higher misorientation angles.[11] In a limited number of experiments substrates with a misorientation of 2° toward the *m*-sapphire plane were coloaded for comparison with substrates misoriented toward *a* plane. In the following the notation 2A (2° toward the *a*-sapphire plane), 4A (4° toward the *a*-sapphire plane), 2M (2° toward the *m*-sapphire plane), etc. will be used to identify the samples grown on the different substrates. All samples were fabricated by MOCVD using trimethylgallium (TMGa), trimethylaluminum (TMAl), trimethylindium (TMIn), and ammonia as precursors. Si_2H_6 was used as *n*-type dopant. The growth was initiated with the deposition of an ~1.5 μm thick GaN layer following the procedure described in Ref. 11. For all InGaN/GaN MQW samples, the GaN base layer was doped with silicon resulting in a free carrier concentration of about 1×10^{18} cm^{-3}. Five period $In_xGa_{1-x}N/GaN$ MQW stacks comprised of 2.5–2.8

[a]Electronic mail: stacia@ece.ucsb.edu.

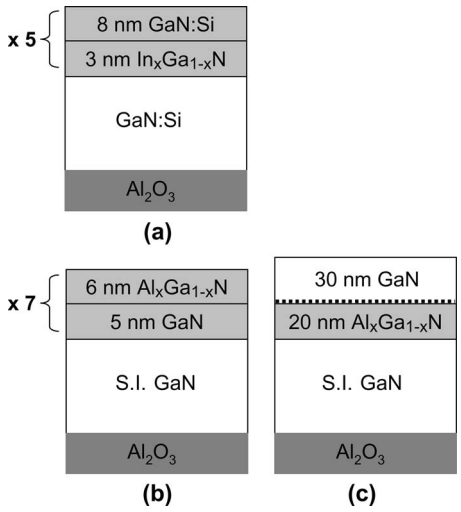

FIG. 1. Schematic structures of the investigated samples.

nm thick $In_xGa_{1-x}N$ wells and 8 nm thick GaN:Si barriers ($n \sim 1 \times 10^{18}$ cm^{-3}) were deposited at temperatures between 890–920 °C at a chamber pressure of 500 Torr. The TMGa and NH_3 flows during MQW growth amounted to 4 and 0.22 mol/min, respectively. The TMIn flow was varied between 3 and 8 μmol/min. The InGaN wells and 1.2 nm of the following barrier layer were grown using N_2 as carrier gas. 1 l/min of H_2 was added to the gas mixture for the growth of the following 6 nm of the barrier layer to mitigate the formation of hexagonal surface features during MQW growth.[13] The H_2 flow was turned off again during the growth of the last 0.8 nm of each barrier.

To enable their electrical characterization, for the AlGaN/GaN heterostructures the 1.4 μm GaN base layers were rendered semi-insulating (S.I.) through Fe doping using bis-cyclopentadienyl iron as described in Ref. 12. On top of the Fe-doped layer, a 0.15 μm thick unintentionally doped spacer layer was deposited with $f_{TMGa}=50$ μmol/min and $f_{NH_3}=270$ mmol/min to separate the Fe-doped base and the active region of the layer structure. Afterwards, the growth temperature was lowered to 1145 °C for the deposition of (a) 7 period MQWs consisting of 5 nm thick GaN wells and 6 nm thick $Al_xGa_{1-x}N$ barriers and (b) 18–25 nm thick $Al_xGa_{1-x}N$ layers followed by a 30 nm GaN cap layer. Both structures were grown using TMGa flows between 6.8 and 8.5 μmol/min, TMAl flows between 3 and 5 μmol/min and 0.18 mol/min NH_3. The reactor pressure was kept constant at 100 Torr. To evaluate the surface/interface properties, additional samples were fabricated, where the growth was stopped after the deposition of the 18–25 nm thick $Al_xGa_{1-x}N$ layers. The schematic sample structures are illustrated in Fig. 1.

The growth rate and composition of the (Al,Ga,In)N layers grown under the various conditions were determined from the analysis of x-ray diffraction (XRD) ω-2θ scans across the (0004) reflection of the MQW samples taken with a Panalytical MRD Pro diffractometer.[14] Room temperature (RT) photoluminescence (PL) spectra were recorded using the 325 nm line of a He–Cd laser with an excitation density of 220 mW/cm^2. All atomic force microscopy (AFM) images were taken with a Digital Instruments Dimension 3100 instrument, operated in tapping mode. The root mean square (rms) surface roughness was calculated using the AFM software. The electrical properties of the two-dimensional electron gas (2DEG), which formed at the upper GaN/AlGaN interface of the S.I. GaN/AlGaN/GaN samples, were evaluated using van der Pauw–Hall measurements and transfer length method (TLM) measurements.

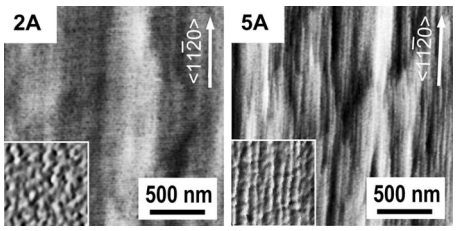

FIG. 2. AFM images of 5 period (2.8 nm InGaN/ 8 nm GaN) MQW samples grown at 905 °C on substrates with misorientation angles of (left) 2° and (right) 5° toward the *a*-sapphire plane. The rms values were 0.5 and 0.9 nm, respectively (grayscale=10 nm). The inserts are fourfold enlargements in amplitude mode (grayscale=0.1 V).

III. RESULTS

A. InGaN/GaN multiquantum wells

The AFM images in Fig. 2 illustrate the surface morphology of InGaN/GaN MQW samples grown at 905 °C on 2A and 5A substrates. While the 2A sample was rather smooth (rms=0.47 nm) and no distinct surface steps were visible, the 5A sample showed surface undulations parallel to the $\langle 11\bar{2}0 \rangle_{GaN}$ direction, which we attribute to step bunching during the growth of the InGaN layers.[11] Note that the average terrace width observed in the AFM image (~20 nm) was significantly larger than the width expected for steps with a height of 0.26 nm as seen on Ga-polar GaN,[15] which would result in a terrace width of 3 nm on 5° misoriented substrates, far below the lateral resolution of the AFM instrument. The observed terrace width of about 20 nm corresponded to the formation of multiatomic steps with a step height in the order of 3–4 unit cells (i.e., ~6–8 GaN monolayers). Multiatomic steps were also observed on the 4A samples (not shown). Thereby the tendency toward step bunching at higher misorientation angles was not always reflected in the overall surface roughness of the samples, which was influenced not only by the multiatomic steps but also by surface undulations with a period of about 1 μm, resulting in similar roughness values for GaN films and heterostructure samples as illustrated in Fig. 3. As expected, the differences in the surface/interface morphology strongly affected the XRD spectra of the MQW samples. Figure 4 displays the ω-2θ scans across the (0004) reflection for InGaN/GaN MQWs grown at 880 °C. For higher intensities the scans were recorded using standard receiving slit optics. With increasing misorientation angle the intensity of the higher order superlattice (SL) peaks strongly decreased, most likely related to the increased interface roughness. In addition, with increasing misorientation angle the main SL peak moved closer to the GaN base layer peak, while the spacing of the SL peaks stayed approximately constant. More detailed

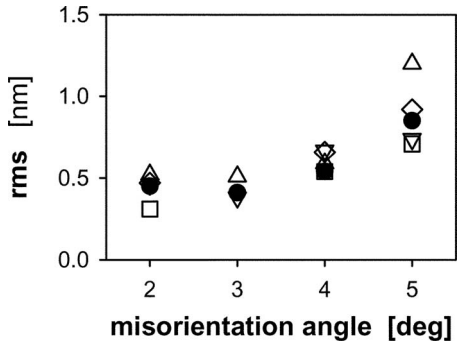

FIG. 3. Dependence of the rms roughness of 2×2 μm^2 AFM images on the substrate misorientation angle for (●) 1.5 μm thick GaN layers, 5 period (2.8 nm InGaN/ 8 nm GaN) MQWs grown at 905 °C with (◇) 3 μmol/min and (□) 8 μmol/min TMIn, (△) 30 nm $Al_{0.2}Ga_{0.8}N$, and (▽) 26 nm $Al_{0.32}Ga_{0.68}N$ grown on top of 1.5 μm thick GaN layers.

analysis of the spectra revealed that while the well and barrier thicknesses were about the same for all samples, the indium mole fraction x_{In} in the $In_xGa_{1-x}N$ wells decreased from 0.17 (2A) to 0.12 (5A) with increasing misorientation angle. For the same samples, the emission wavelength of the MQW related luminescence peak determined in the RT PL measurements shifted from 2.72 to 2.94 eV (Fig. 5). The shift toward higher emission energies with increasing substrate misorientation angle was observed in the entire InGaN growth parameter range investigated in this study. Thereby the intensity of the MQW related luminescence generally increased with increasing misorientation angle, even for small variations in the indium mole fraction as illustrated in Fig. 6 for samples grown at 905 °C. Interestingly, the luminescence intensity recorded for 2M samples, which were coloaded in selected experiments for comparison, always surpassed those recorded for the 5A samples (Fig. 6). Thereby the surface morphology of the 2M samples observed in 2×2 μm AFM images was indistinguishable from those of the corresponding 2A samples. In addition, no significant differences were seen in the XRD scans or the MQW emission wavelength of 2A and 2M samples.

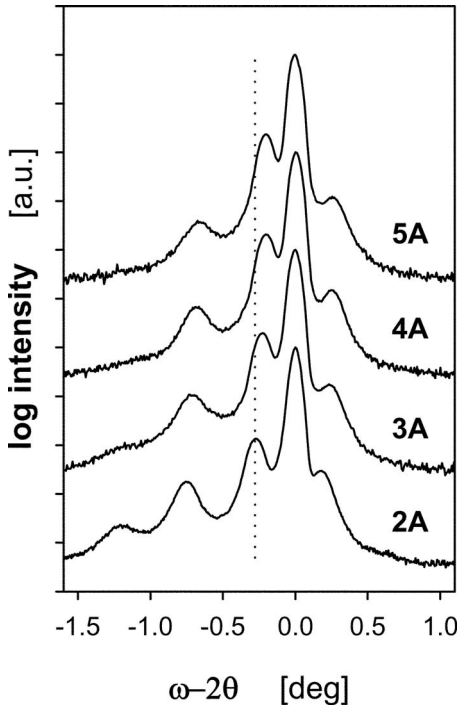

FIG. 4. $(000\bar{4})$ reflection ω-2θ XRD scans recorded using standard receiving slit optics for 5 period N-polar (2.8 nm InGaN/ 8 nm GaN) MQW samples grown on substrates with different misorientation angles.

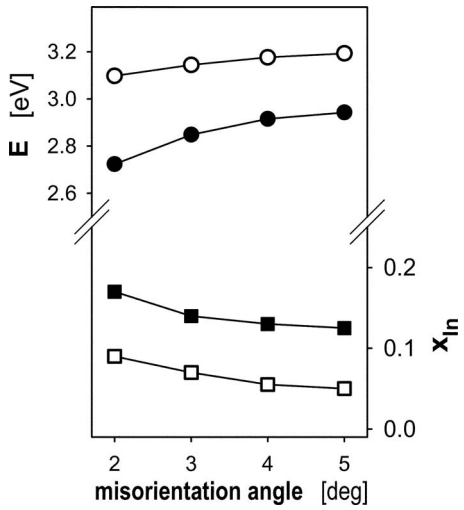

FIG. 5. Dependence of the emission energy of the MQW related luminescence peak at 300 K (circles) and the indium mole fraction in the $In_xGa_{1-x}N$ well, x_{In}, determined by high-resolution XRD (squares) on the substrate misorientation angle for 5 period (InGaN/GaN) MQWs grown at 880 °C (filled symbols) and 905 °C (open symbols).

B. AlGaN/GaN heterostructures

Figure 7 displays the surface morphology of 25 nm thick $Al_{0.32}Ga_{0.68}N$ layers grown on 2A and 5A substrates. On both samples surface steps/undulations parallel to the $\langle 11\bar{2}0\rangle_{GaN}$ direction caused by the misorientation were observed, the density of which increased with increasing misorientation angle resulting in rms roughness values of 0.5 and 0.7 nm for the 2A and 5A samples, respectively. The observed terrace width was ~15 and ~20 nm on the 2A and 5A samples,

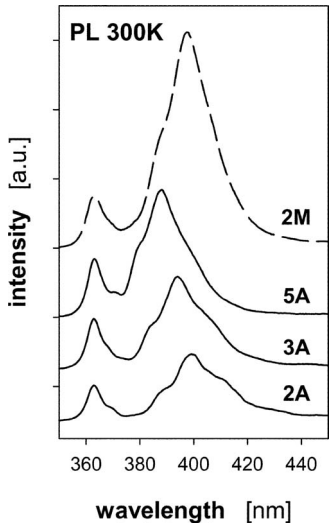

FIG. 6. 300 K PL spectra of 5 period (InGaN/GaN) MQWs grown at 905 °C on substrates with different misorientation angles and misorientation directions.

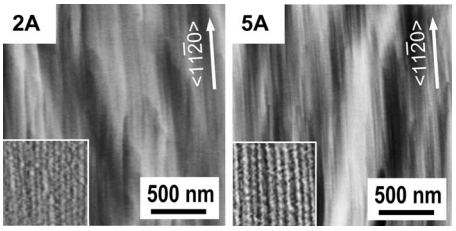

FIG. 7. AFM images of 25 nm thick $Al_{0.32}Ga_{0.68}N$ layers on 1.4 μm GaN grown on substrates with misorientation angles of (left) 2°, rms=0.5 nm and (right) 5°, rms=0.7 nm (grayscale=10 nm). The inserts are fourfold enlargements in amplitude mode (grayscale=0.1 V).

respectively. Both values were again much larger than expected for steps with a height of 0.26 nm [7 nm (2°), 3 nm (5°)] and related to the formation of multiatomic steps, with step heights of about 1 unit cell on the 2A and 3–4 unit cells on the 5A sample. No distinct differences were observed in the rms roughness values for AFM scans recorded on the single heterostructure samples and the AlGaN/GaN MQW samples. In addition, the surface roughness was weakly dependent on the Al mole fraction in the layers (Fig. 3).

In contrast to the observations for InGaN/GaN MQWs, the alloy composition in the AlGaN/GaN MQW structures was not affected by the substrate misorientation angle as seen in Fig. 8 displaying the ω-2θ scans across the (0004) reflection recorded in triple axis mode for a series of 7 $\times$(5.3 nm GaN/6 nm AlGaN) MQW samples. The 2A, 3A, and 4A samples showed distinct MQW related higher order satellite peaks and Pendellösung fringes indicating good periodicity and a high quality of the MQW. The intensity of the higher order SL peaks was somewhat lower for the 5A samples. The intensity decay at higher angles, however, was much less pronounced than that observed for InGaN/GaN MQWs. The PL spectra recorded from the same series of samples are shown in Fig. 9. While the emission wavelength of the MQW related luminescence peak at 384 nm was constant, the luminescence intensity again increased with the increasing misorientation angle. The emission wavelength of 384 nm resulted from the strong polarization fields in the

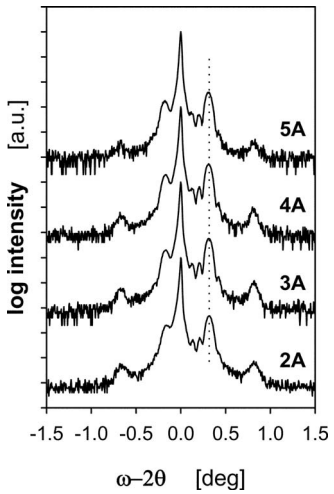

FIG. 8. (0004) reflection ω-2θ XRD scan recorded in triple axis geometry for 7 period N-polar (5 nm GaN / 6 nm $Al_{0.27}Ga_{0.73}N$) MQW samples grown on substrates with different misorientation angles.

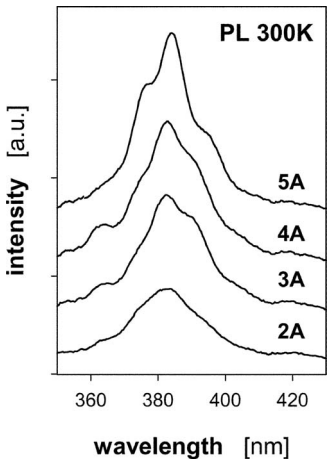

FIG. 9. 300 K PL spectra of 7 period (5 nm GaN / 6 nm $Al_{0.27}Ga_{0.73}N$) MQW samples grown on substrates with different misorientation angles.

MQWs with a GaN well width of 5.3 nm, leading to a significant redshift in the luminescence and a broad full width at half maximum of the emission peaks, similar to the results reported for Ga-polar AlGaN/GaN MQWs.[16,17] No additional measurements, however, were performed to quantify the electric field effects in the N-polar samples.

Figure 10 summarizes the results of the electrical measurements performed on S.I. GaN/ 18 nm $Al_{0.36}Ga_{0.64}N$/30 nm GaN structures grown on substrates with different misorientation angles. All samples exhibited similar sheet carrier densities n_s of about 7.2×10^{12} cm^{-2} determined by Hall and CV measurements. The electron mo-

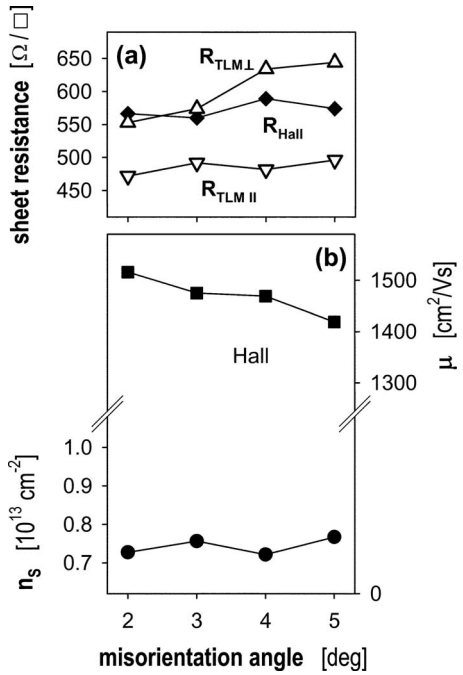

FIG. 10. (a) Dependence of the sheet resistance of the 2DEG measured at 300 K using TLM patterns parallel (triangles down) and perpendicular (triangles up) to the step direction and derived from the van der Pauw–Hall measurements (diamonds) and (b) dependence of the sheet electron concentration (circles) and the electron mobility (squares) determined by van der Pauw–Hall measurements at 300 K on the substrate misorientation angle for 30 nm GaN/ 18 nm $Al_{0.36}Ga_{0.64}N$/S.I. GaN structures.

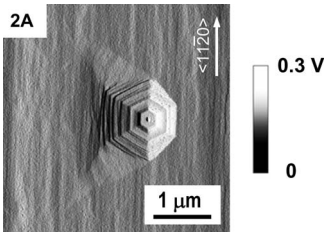

FIG. 11. Amplitude AFM image taken near the edge of a 5 period InGaN/GaN MQW sample grown at 905 °C on a sapphire substrate with a misorientation angle of 2° toward the *a*-sapphire plane.

bility determined in the Hall measurements, however, slightly decreased from 1520 $cm^2/V\,s(2°)$ to 1420 $cm^2/V\,s(5°)$ with the increasing misorientation angle. To study the impact of surface undulations/steps on the properties of the 2DEG, additional TLM patterns were fabricated perpendicular and parallel to the surface undulations/steps. While the resistivity of the 2DEG perpendicular to the surface undulations/step increased from 540 to 645 $\Omega/\square$ with the increasing misorientation angle, the resistivity parallel to the surface undulations/steps, ranging between 470–495 $\Omega/\square$, was significantly lower than those measured in the perpendicular direction and was largely unaffected by the misorientation angle. The electron mobility parallel to the surface steps calculated from the parallel resistivity and the sheet carrier density were as high as 1800 cm^2/Vs. Similar trends were observed for other series of samples, e.g., different Al mole fractions or thicknesses of the AlGaN layer.

IV. DISCUSSION

While the growth on misoriented substrates enabled the growth of smooth N-polar (Al,Ga,In)N films in general, addition of TMAl and lower temperatures as required for InGaN deposition, both parameters which result in a decreased surface mobility of adsorbed species caused the formation of multiatomic steps and surface undulations especially at high misorientation angles (Figs. 2 and 7). Step-bunching effects at high misorientation angles are well known for (Al,Ga,In)(As,P) films.[18] While no detailed model exists for (Al,Ga,In)N growth, step bunching during MOCVD of GaAs is well understood and was associated with differences in molecular dissociation from above and below step edges.[19] Similar to GaN films,[11] no step structure was observed on the surfaces of the InGaN/GaN MQW samples grown on 2A or 2M substrates (Fig. 2). Instead, the surface morphology was characterized by dense, very small depressions, or pits. An investigation of those features is, however, beyond the AFM resolution. On the substrates with small misorientation angles a low mobility of adsorbed species increased the risk of island/hexagon formation. Although all films deposited on substrates with a misorientation angle of 2° were smooth and featureless over large substrate areas near the wafer edges, small hexagons were occasionally observed as shown in Fig. 11 for an InGaN/GaN MQW sample. The defect structure was similar to those observed by Zauner *et al.*[8] No hexagonal features were seen on samples with misorientation angles of 4° and 5°. Interestingly the enhanced formation of multiatomic steps at higher misorientation angles had less impact on the interface quality of the AlGaN/GaN MQWs, which exhibited higher order SL peaks at all angles, in comparison to the InGaN/GaN MQWs where the intensity of higher order SL peaks markedly declined with the increasing misorientation angle. Possibly the stronger effect of the misorientation on the structural properties of the InGaN/GaN MQWs was related to the additional impact of the misorientation on the In composition in the InGaN wells, whereas the alloy composition in the AlGaN layers was unaffected. A similar decrease in the In mole fraction in InGaN layers with the increasing misorientation angle as observed in this study was recently reported for Ga-polar InGaN.[20] Substrate misorientation effects on the incorporation of In into InGaAs layers were reported previously.[21] We speculate that the lower step velocity of the growing film at higher misorientation angles/step densities[22] in conjunction with the low thermal stability of InGaN caused an enhanced indium desorption at lower step velocities. In addition, differences in the incorporation efficiency of indium at the multiatomic steps and on the terraces may play a role in the net indium incorporation in the growing layer. In contrast to the volatile indium, aluminum formed strong bonds with the surface [E_B(Al–N)=2.88 eV; E_B(In–N)=1.93 eV] (Ref. 23) and the Al incorporation efficiency was independent of the substrate misorientation as reflected in the XRD spectra (Fig. 8) and the constant emission wavelength of the AlGaN/GaN MQW related luminescence (Fig. 9). The increase in the luminescence intensity with increasing angle seen for both AlGaN/GaN and InGaN/GaN MQW samples followed the trends observed for the N-polar GaN bulk layers and was related to the decrease in the treading dislocation density in the films with the increasing misorientation angle.[11,24] The reasons for the brighter luminescence observed from 2M in comparison to 2A InGaN/GaN MQW samples, which exhibited similar surface morphologies, MQW properties, and treading dislocation densities as deduced from XRD measurements are not well understood at this time, and further investigations are needed. Possibly differences in the local atomic bonding on the surface of 2M samples enhanced fluctuations in the InGaN alloy composition and carrier localization, reducing nonradiative recombination at threading dislocations. Differences in the impurity concentrations in the InGaN/GaN MQWs cannot be excluded, although no impact of the substrate misorientation on the impurity incorporation was observed for GaN layers grown at higher growth temperatures.[25]

The results of the electrical measurements performed on the S.I. GaN/AlGaN/GaN samples reflected the surface/interface morphology of the samples. While the misorientation did not affect the alloy composition of the AlGaN layers and the sheet carrier density of the 2DEG, which formed at the upper AlGaN/GaN interface, the electron transport properties were markedly anisotropic due to the regular alignment of the surface steps/undulations parallel to the $\langle 11\bar{2}0\rangle$ direction of the (Al,Ga)N crystal, which formed as a consequence of the substrate misorientation. The resistivity of the 2DEG measured perpendicular to the steps/undulations increased from 540 to 645 $\Omega/\square$ with the increasing misorientation angle. Conversely, the resistivity measured parallel to

the steps/undulations was significantly lower (470–495 $\Omega/\square$) and independent of the misorientation angle. Recently a strong anisotropy in the 2DEG properties was observed also for Ga-polar AlGaN/GaN structures grown on vicinal substrates by MBE and associated with an enhanced electron mobility parallel to the steps at the AlGaN/GaN interface due to reduced interface roughness.[26,27] Similar trends were reported for AlGaAs/GaAs heterostructures.[28] The electron mobility of 1800 $cm^2/V\,s$ derived from the sheet resistance and the carrier density for the samples in this study was comparable to the best results reported for group-III polar heterostructures. For device applications, the superior properties of the 2DEG parallel to the steps can be taken advantage of by aligning the devices in such a way that the electron transport occurs parallel to the steps/undulations. Further details related to the impact of the crystal misorientation on the electron transport will be published elsewhere.[29]

V. CONCLUSIONS

Smooth N-polar InGaN/GaN and AlGaN/GaN MQWs and heterostructures were grown by MOCVD on (0001) sapphire substrates with misorientation angles of 2°–5° toward the *a*-sapphire plane. While the indium mole fraction in the InGaN layers decreased with the increasing misorientation angle, the alloy composition of the AlGaN films was unaffected. For all investigated structures the tendency toward formation of multiatomic steps at the film surface and at interfaces increased with the increasing misorientation angle. Thereby multistep formation and surface undulations led to a stronger degradation of the interface quality and periodicity of the InGaN/GaN in comparison to the AlGaN/GaN MQWs. The properties of the 2DEG, which formed at the upper interface of S.I. GaN/AlGaN/GaN heterostructures, were strongly anisotropic. While the resistivity of the 2DEG measured perpendicular to the surface steps/undulations decreased with the increasing misorientation angle, the resistivity measured in the parallel direction was significantly lower and unaffected by the crystal misorientation. Electron mobility values as high as 1800 cm^2/Vs were determined for conduction parallel to the surface steps/undulations.

ACKNOWLEDGMENTS

The authors gratefully acknowledge the support of USAFOSR (Dr. K. Reinhardt and Dr. J. Witt), the ONR-MINE program (Dr. Paul Maki and Dr. Harry Dietrich), and the Solid State Lighting and Energy Center at the University of California Santa Barbara. This research made use of the MRSEC Central Facilities supported by the National Science Foundation.

[1] M. Sumiya, K. Yoshimura, T. Ito, K. Ohtsuka, S. Fuke, K. Mizuno, M. Yoshimoto, H. Koinuma, A. Ohtomo, and M. Kawasaki, J. Appl. Phys. **88**, 1158 (2000).
[2] R. Dimitrov, M. Murphy, J. Smart, W. Schaff, J. R. Shealy, L. F. Eastman, O. Ambacher, and M. Stutzmann, J. Appl. Phys. **87**, 3375 (2000).
[3] F. Bernardini, V. Fiorentini, and D. Vanderbilt, Phys. Rev. B **56**, R10024 (1997).
[4] M. Stutzmann, O. Ambacher, M. Eickhoff, U. Karrer, A. Lima Pimenta, R. Neuberger, J. Schalwig, R. Dimitrov, P. J. Schuck, and R. D. Grober, Phys. Status Solidi B **228**, 505 (2001).
[5] P. Guan, A. L. Cai, J. S. Cabalu, H. L. Porter, and S. Huang, Appl. Phys. Lett. **77**, 2491 (2000).
[6] S. Rajan, A. Chini, M. H. Wong, J. S. Speck, and U. K. Mishra, J. Appl. Phys. **102**, 044501 (2007).
[7] M. H. Wong, S. Rajan, R. M. Chu, T. Palacios, C. S. Suh, L. S. McCarthy, S. Keller, J. S. Speck, and U. K. Mishra, Phys. Status Solidi A **204**, 2049 (2007).
[8] A. R. A. Zauner, J. L. Weyher, M. Plomp, V. Kirilyuk, I. Grzegory, W. J. P. van Enckevort, J. J. Schermer, P. R. Hageman, and P. K. Larsen, J. Cryst. Growth **210**, 435 (2000).
[9] A. R. A. Zauner, A. Aret, W. J. P. van Enckevort, J. L. Weyher, S. Porowski, and J. J. Schermer, J. Cryst. Growth **240**, 14 (2002).
[10] T. Matsuoka, Y. Kobayashi, H. Takahata, T. Mitate, S. Mizuno, A. Sasaki, M. Yoshimoto, T. Ohnishi, and M. Sumiya, Phys. Status Solidi B **243**, 1446 (2006).
[11] S. Keller, N. A. Fichtenbaum, F. Wu, A. Rosales, S. P. DenBaars, J. S. Speck, and U. K. Mishra, J. Appl. Phys. **102**, 083546 (2007).
[12] S. Keller, C. S. Suh, Z. Chen, R. Chu, S. Rajan, N. A. Fichtenbaum, M. Furukawa, S. P. DenBaars, J. S. Speck, and U. K. Mishra, J. Appl. Phys. **103**, 033708 (2008).
[13] S. Keller, N. A. Fichtenbaum, M. Furukawa, J. S. Speck, S. P. DenBaars, and U. K. Mishra, Appl. Phys. Lett. **90**, 191908 (2007).
[14] O. Brandt, P. Waltereit, and K. H. Ploog, J. Phys. D **35**, 577 (2002).
[15] D. Kapolnek, X. H. Wu, B. Heying, S. Keller, B. P. Keller, U. K. Mishra, S. P. DenBaars, and J. S. Speck, Appl. Phys. Lett. **67**, 1541 (1995).
[16] N. Grandjean, B. Damilano, S. Dalmasso, M. Leroux, M. Laügt, and J. Massies, J. Appl. Phys. **86**, 3714 (1999).
[17] M. D. Craven, P. Waltereit, J. S. Speck, and S. P. DenBaars, Appl. Phys. Lett. **84**, 496 (2004).
[18] J. Ishizaki, S. Goto, M. Kishida, T. Fukui, and H. Hasegawa, Jpn. J. Appl. Phys., Part 1 **33**, 721 (1994).
[19] A. L.-S. Chua, E. Pelucchi, A. Rudra, B. Dwir, E. Kapon, A. Zangwill, and D. D. Vvendensky, Appl. Phys. Lett. **92**, 013117 (2008).
[20] M. Kryśko, G. Franssen, T. Suski, M. Albrecht, B. Łucznik, I. Grzegory, S. Krukowski, R. Czernecki, S. Grzanka, I. Makarowa, M. Leszyński, and P. Perlin, Appl. Phys. Lett. **91**, 211904 (2007).
[21] J. te Nijenhuis, P. R. Hageman, and L. J. Giling, J. Cryst. Growth **167**, 397 (1996).
[22] R. M. Lum, J. K. Klingert, D. W. Kisker, S. M. Abys, and F. A. Stevie, J. Cryst. Growth **93**, 120 (1988).
[23] *Properties of Group-III Nitrides*, edited by J. H. Edgar (INSPEC, New York, 1994).
[24] T. Sugahara, H. Sato, M. Hao, Y. Naoi, S. Kurai, S. Tottori, K. Yamashita, K. Nishino, L. T. Romano, and S. Sakai, Jpn. J. Appl. Phys., Part 2 **37**, L398 (1998).
[25] N. A. Fichtenbaum, T. A. Mates, S. Keller, S. P. DenBaars, and U. K. Mishra, J. Cryst. Growth **310**, 1124 (2008).
[26] X. Q. Shen, H. Okumura, K. Furuta, and N. Nakamura, Appl. Phys. Lett. **89**, 171906 (2006).
[27] N. Nakamura, K. Furuta, X. Q. Shen, T. Kitamura, K. Nakamura, and H. Okumura, J. Cryst. Growth **301–302**, 452 (2007).
[28] Y. Nakamura, T. Noda, J. Motohisa, and H. Sakaki, Physica E (Amsterdam) **8**, 219 (2000).
[29] S. Rajan, S. Keller, E. Hsieh, S. P. DenBaars, J. S. Speck, and U. K. Mishra (unpublished).